Electronic Supplementary Information

Synthesis of bare Pt_3Ni nanorod from PtNi@Ni core-shell nanorod by acid etching: one step surfactant removal and phase conversion for optimal electrochemical performance toward oxygen reduction reaction

Jisun Yoon,[b] Jongsik Park,[ab] Young Jin Sa,[c] Yoojin Yang,[b] Hionsuck Baik,[d] Sang Hoon Joo*[ce], and
Kwangyeol Lee*[a]

[a]Center for Molecular Spectroscopy and Dynamics, Institute for Basic Science (IBS), Seoul 02841, Korea.

[b]Department of Chemistry and Research Institute of Natural Sciences, Korea University, Seoul 02841, Korea.

[c]Department of Chemistry and School of Energy and Chemical Engineering, Ulsan National Institute of Science and Technology (UNIST), Ulsan 44919, Korea

[d]Korea Basic Science Institute (KBSI), Seoul 02841, Korea.

[e]School of Energy and Chemical Engineering, Ulsan National Institute of Science and Technology (UNIST), Ulsan 44919, Korea.

* Corresponding author: kylee1@korea.ac.kr (K. Lee), shjoo@unist.ac.kr (S. H. Joo)

Material Characterizations

Transmission electron microscopy (TEM) and high-resolution TEM were performed on a TECNAI G2 20 S-Twin operated at 200 kV and TECNAI G2 F30 operated at 300 kV. Elemental mapping and energy dispersive X-ray spectra (EDX) were obtained with a FEI Titan Cubed 60-300 with Chemi-STEM technology and a JEOL ARM200F Cs STEM. X-ray diffraction (XRD) patterns were collected with a Rigaku Ultima III diffractometer system using a graphite-monochromatized Cu-Kα radiation at 40 kV and 30 mV. The electrochemical experiment was performed using a CHI model 660d potentiostat (CH Instruments, Austin, TX). Infrared spectroscopy (IR) were performed on a Microscopic FT-IR/Raman Spec. (Vertex 80V, Bruker, Germany).

Experimental Section

Preparation of PtNi@Ni nanorod. A slurry of Pt(acac)$_2$ (0.15 mmol, Aldrich, 97%), Ni(acac)$_2$ (0.9 mmol, Aldrich, 95%), 1,2-hexadecanediol (0.40 mmol, Aldrich, 90%) was dissolved in oleylamine (6 mL, Aldrich, 70%) and then added into a 100 mL schlenk tube. First, the mixture was aged at 80 ^{o}C with magnetic stirring under Ar for 5 hours and it turned to dark bluish-green. Second, the aged mixture was re-purged with CO and heated up to 230 ^{o}C with maximum voltage for 10 min. The black product after being cooled down to room temperature was purified by washing with methanol/toluene. The resulting precipitates were further purified 2 times by washing with methanol/toluene (v/v = 7/1).

Preparation of Pt$_3$Ni nanorod/C (PNRC) catalyst from PtNi@Ni nanorod. The prepared 30 mg PtNi@Ni nanorod was supported on 120 mg carbon black with sonication. The prepared 50 mg of PtNi@Ni/C catalysts were dispersed in 10 mL ethanol and 30 mL acetic acid, and the mixed solution was sonicated for 2 h. The final product was purified by washing with acetone for three times.

Preparation of Pt$_3$Ni nanorod/C (PNR) catalyst. The Pt$_3$Ni nanorod/C (PNR) was prepared by modifying previous study of our group.[1] A slurry of Pt(acac)$_2$ (0.06 mmol), Ni(acac)$_2$ (0.02 mmol), ethylene glycol (1.86 mmol) and octadecylamine (15 mmol) was prepared in a 15 mL two-neck round bottom flask with magnetic stirring. After being evacuated for 120 min with stirring at 80 ^{o}C, the resulting solution was charged by CO gas and then heated up to 150 ^{o}C, and kept at that temperature for 120 min under CO gas. Finally, dark brown precipitates could be obtained by cooling down the solution to room temperature and then by centrifugation with added methanol / toluene (v/v = 15 mL/ 15 mL). The prepared 30 mg Pt$_3$Ni nanorod was supported on 120 mg carbon black with sonication. The prepared 50 mg of Pt$_3$Ni nanorod/C catalysts were dispersed in 10 mL ethanol and 30 mL acetic acid, and the mixed solution was sonicated for 2 h. The final product was purified by washing with acetone for three times.

Material Characterizations. Transmission electron microscopy (TEM) and high-resolution TEM were performed on a TECNAI G2 20 S-Twin operated at 200 kV and TECNAI G2 F30 operated at 300 kV. Elemental mapping and energy dispersive X-ray spectra (EDX) were obtained with a FEI Titan Cubed 60-300 with Chemi-STEM technology and a JEOL ARM200F Cs STEM. X-ray diffraction (XRD) patterns were collected with a Rigaku Ultima III diffractometer system using a graphite-monochromatized Cu-Kα radiation at 40 kV and 30 mV. The electrochemical experiment was performed using a CHI model 660d potentiostat (CH Instruments, Austin, TX). Infrared spectroscopy (IR) were performed on a Microscopic FT-IR/Raman Spec. (Vertex 80V, Bruker, Germany).

Electrochemical characterization. Electrocatalytic activity of the samples was evaluated using CHI760E electrochemical working station with an electrode rotator (PINE instrumentation). Glassy carbon (GC) rotating disk electrode, graphite rod, and Ag/AgCl (sat' KCl) were used as working, counter, and reference electrodes, respectively. Before every measurement, the GC electrode was polished on a micro-cloth with alumina aqueous suspension to generate a mirror finish. Catalyst ink was made by mixing catalyst, DI water, Nafion, and ethanol and ultra-sonicating for around 30 min. A certain amount of the resulting ink was dropped onto the GC electrode, and dried. The Pt loading was 14 μg cm^{-2}. Electrochemical measurement was conducted in 0.1 M $HClO_4$, prepared by diluting 70% $HClO_4$ (Veritas Double Distilled, GFS Chemicals) in Millipore water (18.2 MΩ cm). The surface of the catalyst was electrochemically cleaned by 50 potential cycles from 0.05 to 1.2 V (vs. RHE) at 0.5 V s^{-1} in N_2-saturated electrolyte. In the same potential range, cycling voltammogram (CV) was obtained at 50 mV s^{-1} in the same electrolyte to calculate hydrogen under-potential deposition (H_{UPD}) surface area. For Ohmic *iR*-loss correction, electrochemical impedance spectroscopy was measured in a frequency range from 10 kHz (or 100 kHz) to 1 Hz with potential amplitude of 10 mV at 0.68 V (*vs.* RHE). ORR polarization curve was obtained by linear sweep voltammetry from −0.01 to 1.1 V (vs. RHE) in O_2-saturated solution at a rotation speed of 1,600 rpm and at a scan rate of 20 mV s^{-1}. Background current was acquired in the same way, but in N_2-saturated solution. Long-term durability tests were conducted in N_2-saturated 0.1 M $HClO_4$ solution in a potential range from 0.6 to 1.0 V vs. RHE at a scan rate of 50 mV s^{-1} for 20,000 cycles. After the cycling, the ORR activity was measured in fresh electrolyte. The ORR polarization curves before and after potential cycling were obtained under the same conditions as the ones used for the above ORR measurement.

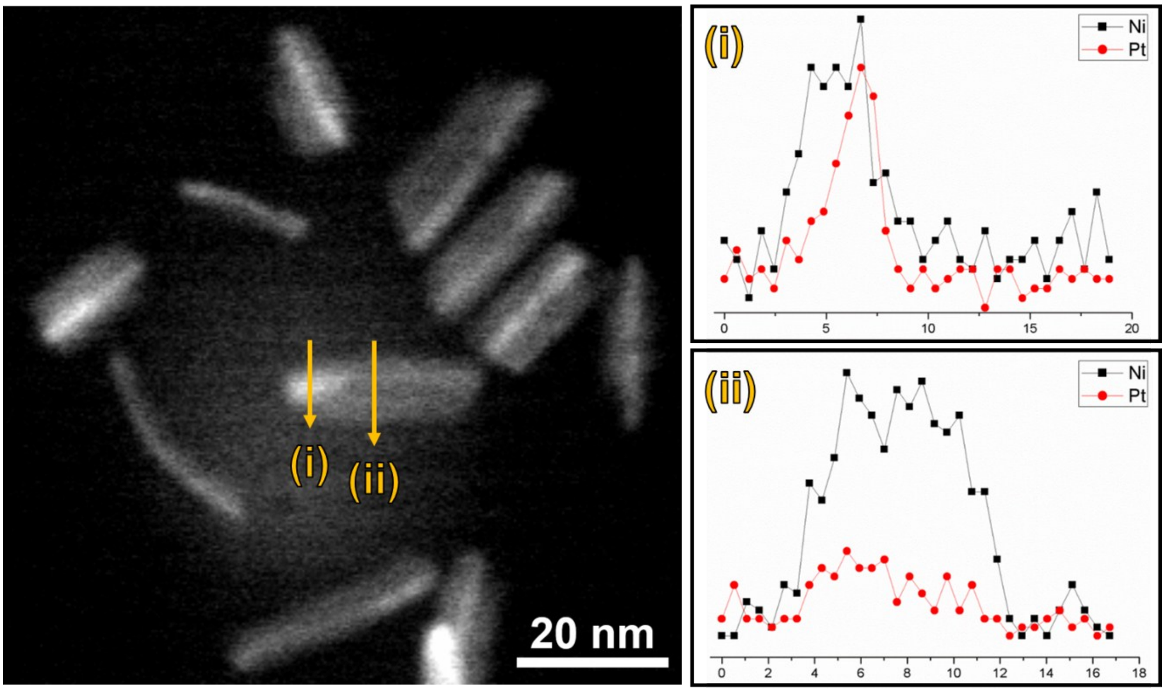

Fig. S1. Line profile analysis of PtNi@Ni nanorod. The bright field in STEM mainly consists of Pt phase.

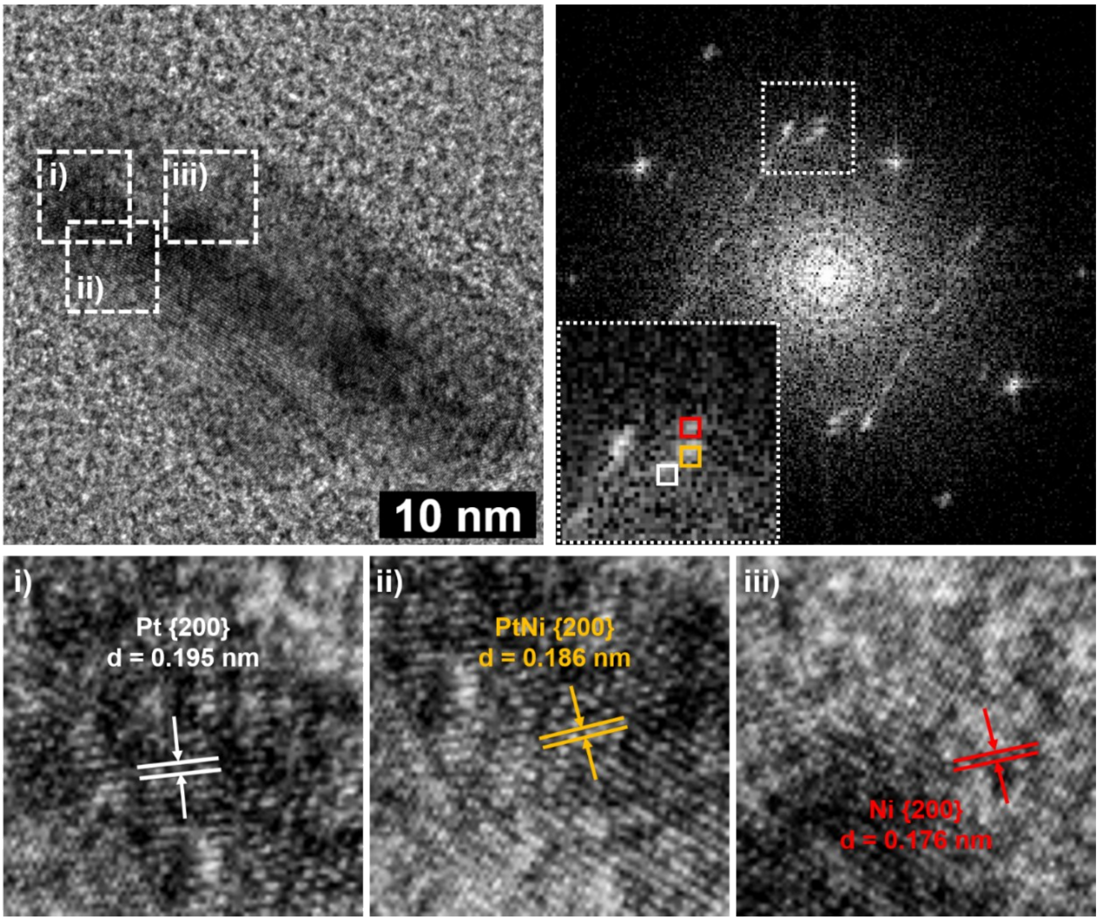

Fig. S2. The enlarged HRTEM image of PtNi@Ni nanorod. Three different segregated phases are clearly seen.

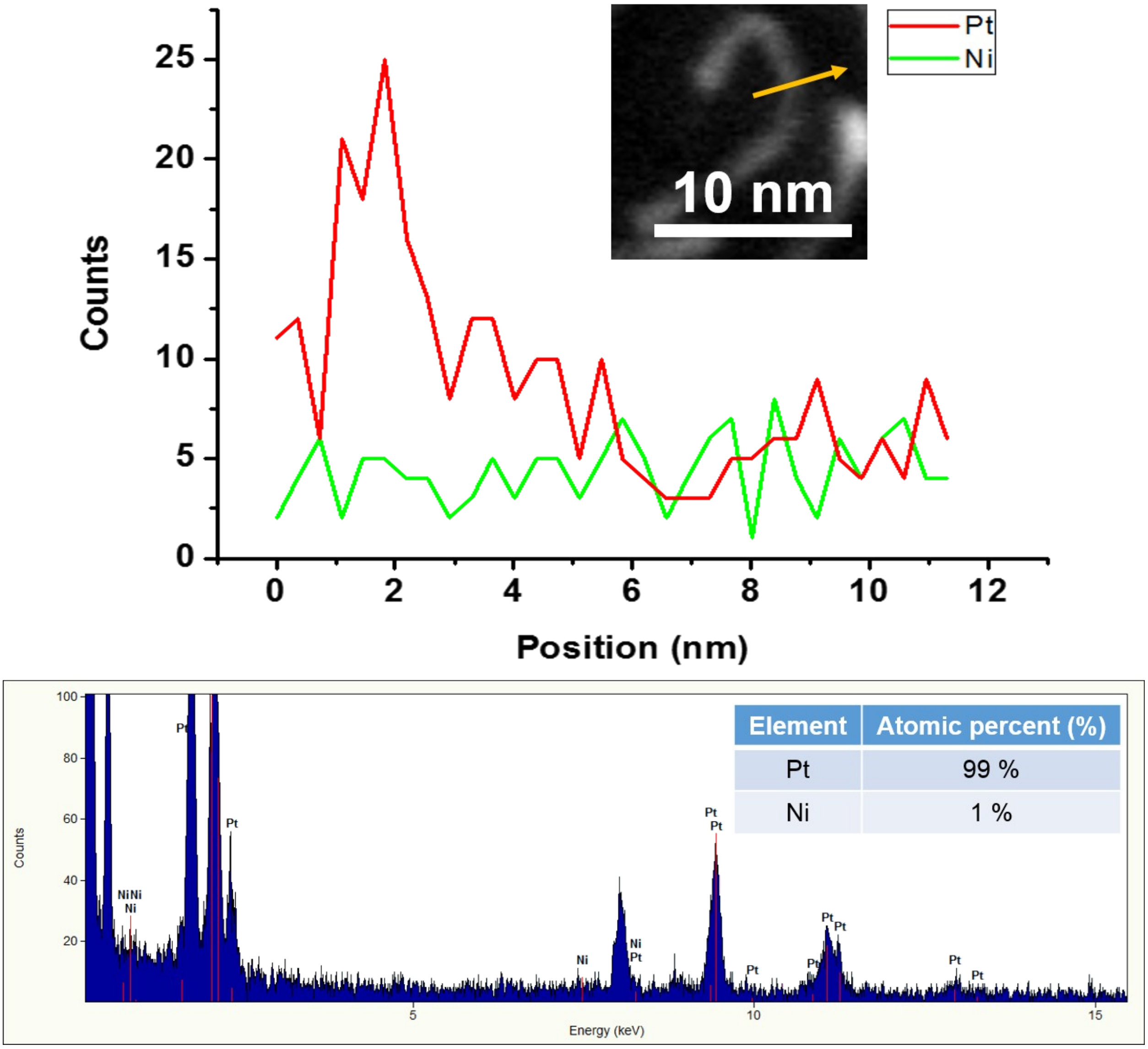

Element	Atomic percent (%)
Pt	99 %
Ni	1 %

Fig. S3. The line profile analysis and EDX analysis of intermediate at 4 min. The composition of intermediates mainly consists of Pt.

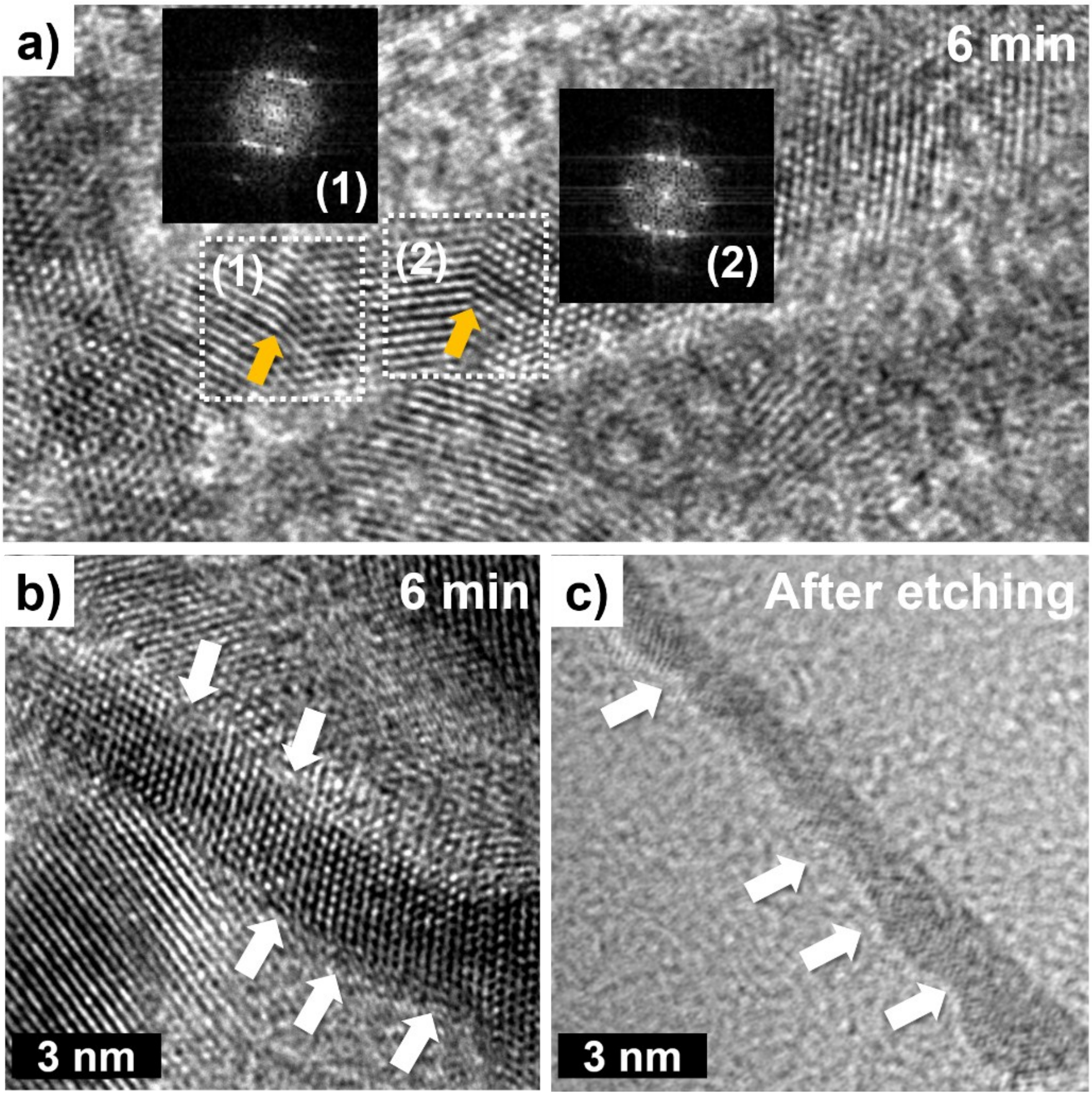

Fig. S4. HRTEM images of a,b) intermediate PtNi nanorod synthesized at 6 min and c) final Pt_3Ni nanorod after acid etching. Yellow arrows indicate the presence of twinning boundaries, and white arrows indicate grooves.

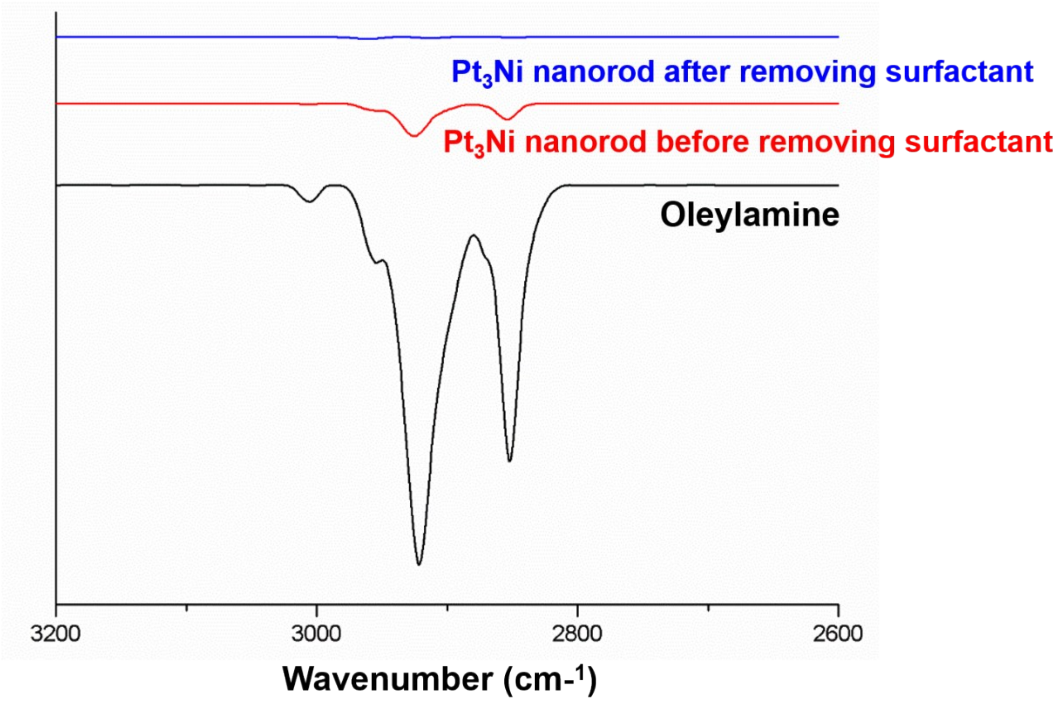

Fig. S5. IR spectra (KBr) of Pt$_3$Ni nanorod before and after removing surfactant, and oleylamine.

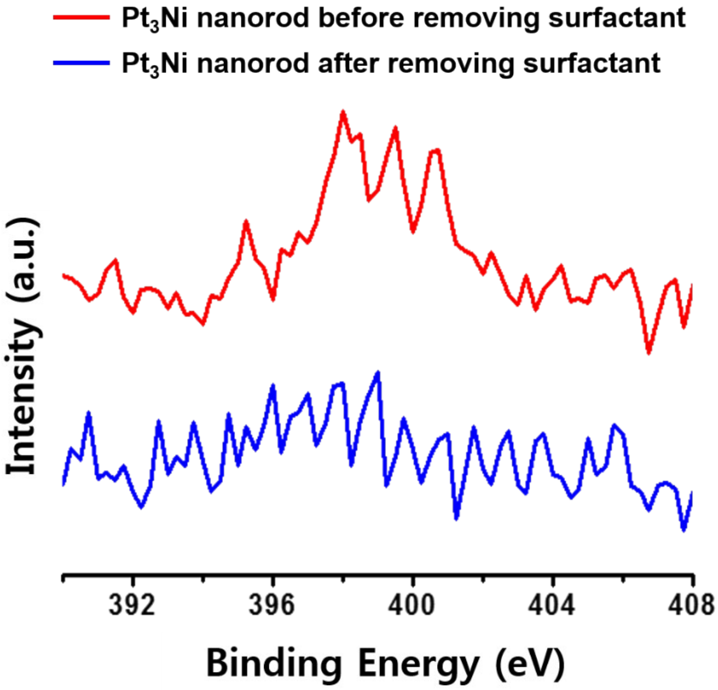

Fig. S6. Nitrogen X-ray photoelectron spectroscopy (XPS) analysis of Pt_3Ni nanorod before and after removing surfactant. The removal of surfactant from Pt_3Ni nanorod is clearly seen.

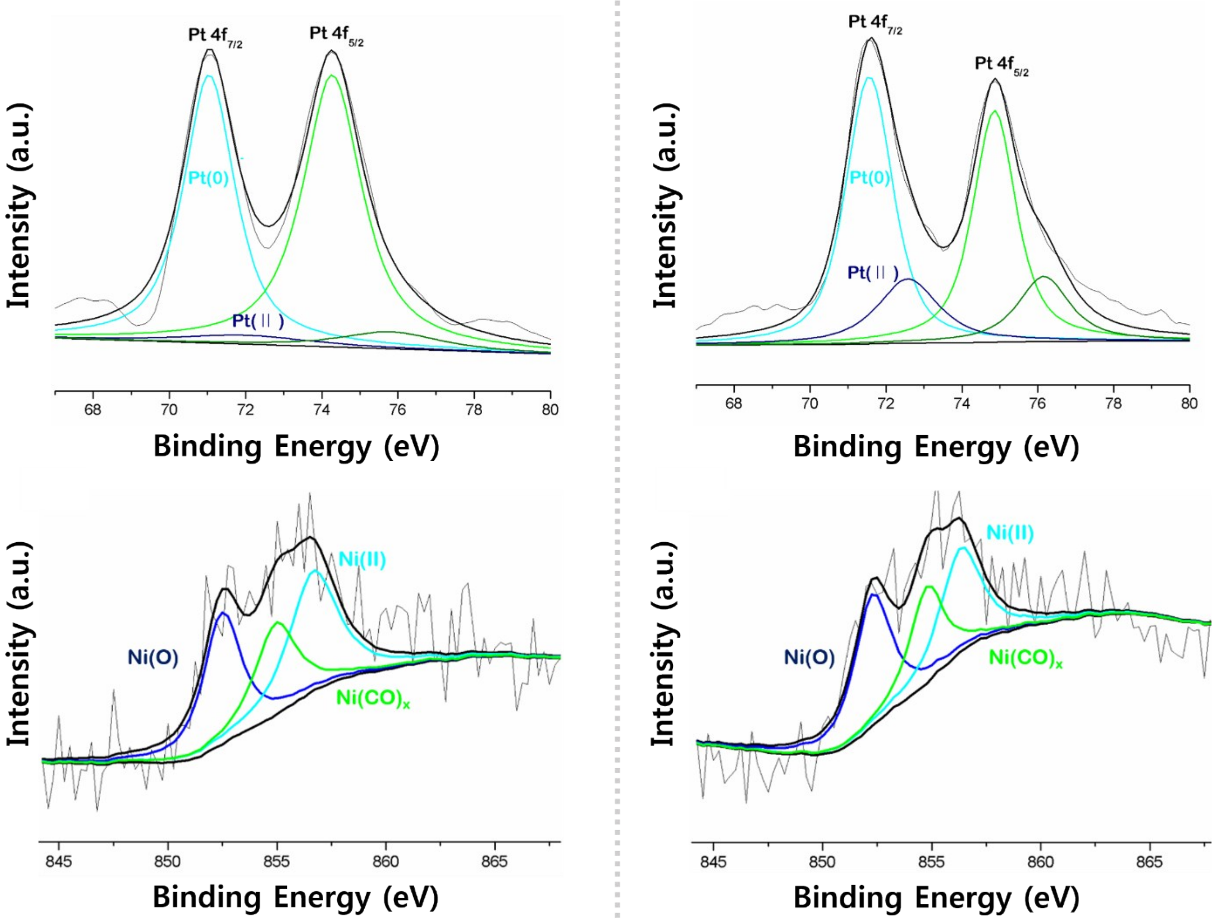

Sample	Species	Binding energy (eV)	Peak Area (%)
PtNi@Ni nanorod	Pt(0)	71.05	92.4
	Pt(II)	72.01	7.6
	Ni(0)	852.48	30.6
	NI(II)	856.66	45.8
	$Ni(CO)_x$	854.94	23.6

Sample	Species	Binding energy (eV)	Peak Area (%)
Pt_3Ni nanorod	Pt(0)	71.56	74.7
	Pt(II)	72.06	25.3
	Ni(0)	852.28	37.5
	NI(II)	856.31	35.6
	$Ni(CO)_x$	854.77	26.9

Fig. S7. X-ray photoelectron spectroscopy (XPS) analysis of PtNi@Ni nanorod and Pt_3Ni nanorod.

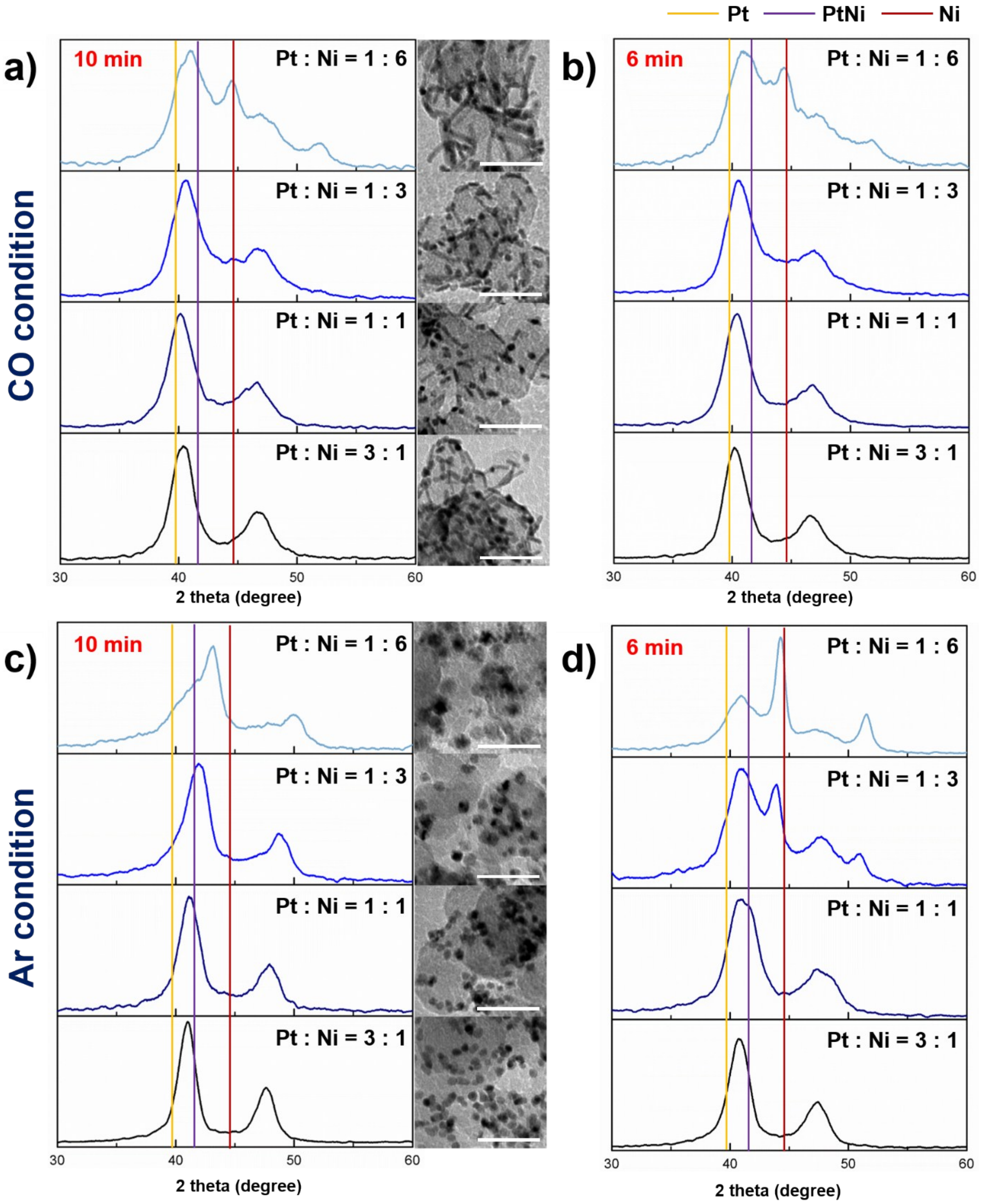

Fig. S8. X-ray diffraction patterns of PtNi alloy nanostructures. Intermediates synthesized at a) 10 min and b) 6 min under CO gas condition. Intermediates synthesized at c) 10 min and d) 6 min under Ar gas condition.

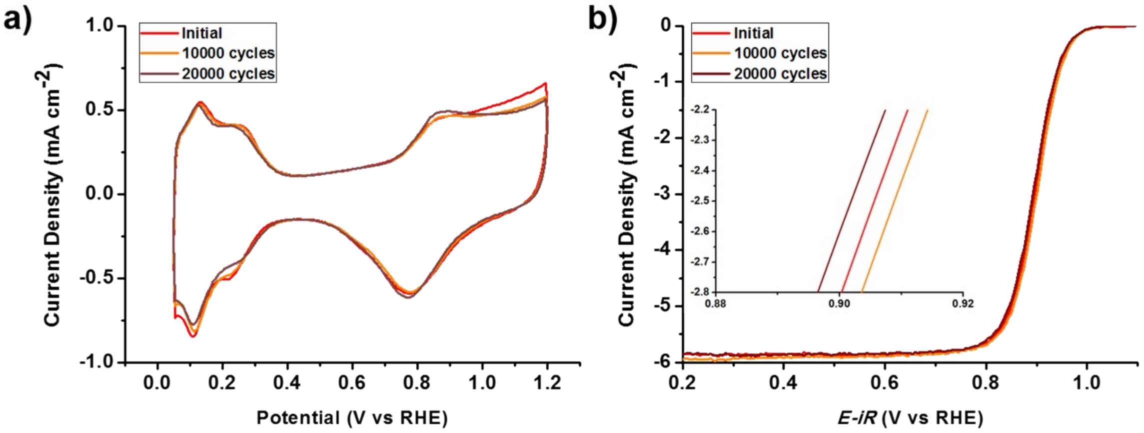

Fig. S9. Electrochemical durability of PNRC. a) Cyclic Voltammograms and b) ORR polarization curves of PNRC.

Table S1. Metal contents from ICP-AES and lattice parameter measured from XRD.

Sample	ICP-AES					XRD	
Reaction time of PtNi NRs	**Pt wt%**	**Pt at%**	**Ni wt%**	**Ni at%**	**Pt : Ni (at%)**	**Lattice parameter (nm)**	**Contraction of lattice parameter vs Pt (%)**
Reference Pt	-		-		-	0.3919	0
6 min (PtNi NRs)	61.76	**50.8**	17.98	**49.2**	**1:1**	0.3870	1.3
10 min (PtNi@Ni NRs)	31.46	**13.6**	59.80	**86.3**	**1:6.3**	0.3845	1.9

Table S2. Metal contents from ICP-AES of PNRC and PNR.

Sample	Pt (wt%)	Ni(wt%)	Molar ratio (Pt:Ni)
PNRC	16.3	1.6	3.63 :1
PNR	13.1	1.4	2.81 : 1

References

[1] N. T. Khi, H. Baik, H. K. Lee, J. Yoon, J. –H. Sohn and K. Lee, *Nanoscale*, 2014, **6**, 11007.